HHS Public Access

Author manuscript

Nature. Author manuscript; available in PMC 2012 October 05.

Published in final edited form as:

Nature. ; 484(7392): 125–129. doi:10.1038/nature10936.

Small-molecule inhibitors of the AAA+ ATPase motor cytoplasmic dynein

Ari J. Firestone[1,*], **Joshua S. Weinger**[2,*], **Maria Maldonado**[2], **Kari Barlan**[3], **Lance D. Langston**[2], **Michael O'Donnell**[2], **Vladimir I. Gelfand**[3], **Tarun M. Kapoor**[2], and **James K. Chen**[1]

[1]Department of Chemical and Systems Biology, Stanford University School of Medicine, Stanford, CA 94305

[2]Rockefeller University, New York City, NY 10021

[3]Department of Cell and Molecular Biology, Northwestern University School of Medicine, Chicago, IL 60611

Abstract

The conversion of chemical energy into mechanical force by AAA+ (ATPases associated with diverse cellular activities) ATPases is integral to cellular processes, including DNA replication, protein unfolding, cargo transport, and membrane fusion[1]. The AAA+ ATPase motor cytoplasmic dynein regulates ciliary trafficking[2], mitotic spindle formation[3], and organelle transport[4], and dissecting its precise functions has been challenging due to its rapid timescale of action and the lack of cell-permeable, chemical modulators. Here we describe the discovery of ciliobrevins, the first specific small-molecule antagonists of cytoplasmic dynein. Ciliobrevins perturb protein trafficking within the primary cilium, leading to their malformation and Hedgehog signaling blockade. Ciliobrevins also prevent spindle pole focusing, kinetochore-microtubule attachment, melanosome aggregation, and peroxisome motility in cultured cells. We further demonstrate the ability of ciliobrevins to block dynein-dependent microtubule gliding and ATPase activity *in vitro*. Ciliobrevins therefore will be useful reagents for studying cellular processes that require this microtubule motor and may guide the development of additional AAA+ ATPase superfamily inhibitors.

Correspondence and requests for materials should be addressed to J.K.C. (jameschen@stanford.edu) or T.M.K. (kapoor@rockefeller.edu).

*These authors contributed equally to this work.

Author Information: Reprints and permissions information is available at www.nature.com/reprints.

Author Contributions: J.K.C. and T.M.K. conceived and directed the study. A.J.F. performed chemical syntheses and assays of Hedgehog signaling, primary cilia formation and function, ATPase activity, vanadate-dependent dynein photocleavage, and p97-dependent protein degradation. A.J.F. and M.M. performed mitotic spindle analyses. K.B. and V.I.G. designed and interpreted the melanophore and peroxisome trafficking assays. J.S.W. performed microtubule gliding and dynein/microtubule binding assays. L.D.L. and M.O. designed and interpreted the Mcm2-7 helicase assays. A.J.F. and J.K.C. wrote the manuscript with contributions from all other authors.

The authors declare no competing financial interests.

Supplementary Information is available online.

Readers are welcome to comment on the online version of this article at www.nature.com/nature.

The AAA+ superfamily of enzymes couples ATP hydrolysis with the generation of mechanical force to regulate diverse aspects of prokaryote and eukaryote biology[1]. ATP-dependent conformational changes can propagate through these molecular machines to complete cellular processes within seconds, and chemical inhibitors that act rapidly and reversibly are much-needed tools for investigating the cellular functions of individual superfamily members. Yet to date only one AAA+ ATPase mechanoenzyme has been selectively targeted by a small molecule[5].

We recently conducted a high-throughput screen for inhibitors of the Hedgehog (Hh) pathway (Fig. 1a)[6], a key mediator of embryonic development and oncogenesis[7]. Our study was designed to identify compounds that act downstream of Smoothened (Smo), a transmembrane Hh signaling protein, and one of the small molecules, HPI-4 (Fig. 1b; **1**), blocked Hh pathway activation in cells lacking the negative regulator Suppressor of Fused (Sufu)[6]. Prolonged treatment of cells with this benzoyl dihydroquinazolinone also reduced the number and size of primary cilia, a microtubule-based extension of the plasma membrane that is required for Hh signaling[8]. Intrigued by these cellular phenotypes, we investigated the biochemical mechanism of HPI-4.

We first synthesized a series of analogs (Fig. 1b; **2-9**) and evaluated their effects on Hh signaling and primary cilia formation (Fig. 1, c-d, and Supplementary Figs. 1-3). Chemical derivatives lacking either a 3- or 4-chloro substituent on the benzoyl ring system (**2** and **6**) or the acyclic ketone (**9**) were significantly less active in either assay (Fig. 1, b and d). The other small molecules segregated into 2,4-dichlorobenzoyl dihydroquinazolinones that inhibit both Hh signaling and primary cilia formation (**1, 3-5**), which we henceforth name “ciliobrevins A-D,” and monochlorobenzoyl analogs that can block Hh target gene expression without inducing ciliary defects (**7** and **8**) (Fig. 1, b and d).

Hh signaling is primarily mediated by the transcription factors Gli2 and Gli3, which exist in a pathway state-dependent balance of N-terminal repressors (Gli2/3R), full-length polypeptides (Gli2/3FL), and transcriptional activators (Gli2/3A) (Fig. 1a)[7]. Both repressor and activator formation require the primary cilium[8], and accordingly ciliobrevins altered the Gli3FL/Gli3R ratio in cells stimulated with the N-terminal domain of Sonic Hedgehog (Shh-N) (Fig. 1e; 30 μM doses of each compound). Shh-N-dependent Gli3FL phosphorylation was also reduced by these compounds, perhaps reflecting loss of Gli3A[9]. In contrast, none of the other analogs had a significant effect on the Gli3 processing or phosphorylation state (Fig. 1e).

To better understand the basis of these phenotypes, we took advantage of the temporal control afforded by chemical perturbations. While prolonged exposure to these compounds causes defects in axonemal morphology, shorter treatments can divulge ciliobrevin-sensitive processes within structurally intact cilia. Since Hh pathway activation coincides with Gli2 accumulation at the distal ciliary tip[10], we examined the effect of ciliobrevins on Gli2 localization (Fig. 1f). We incubated Hh-responsive cells with individual compounds at a 30-μM concentration in the absence or presence of Shh-N-conditioned medium for 4 hours. Gli2 localization was unchanged by derivatives that do not significantly perturb ciliogenesis

(**2** and **8**), whereas ciliobrevins A and D (**1** or **5**) induced ciliary Gli2 levels comparable to that in Shh-N-stimulated cells.

The ability of ciliobrevins to increase ciliary Gli2 levels suggests that these compounds might target protein trafficking mechanisms within this organelle. Intraflagellar transport (IFT) can be resolved into anterograde trafficking, which requires the plus end-directed motor kinesin-2 and the IFTB multisubunit complex, and retrograde trafficking, which utilizes the minus end-directed motor cytoplasmic dynein 2 and the IFTA complex[8]. Loss of the primary cilia-specific cytoplasmic dynein 2 heavy chain (Dync2h1) alters cilia morphology[11], reduces Hh target gene expression[11], and increases ciliary levels of Gli2[10]. Similarities between these genetic phenotypes and the effects of ciliobrevins led us to hypothesize that these small molecules might inhibit cytoplasmic dynein 2. We therefore examined the effect of ciliobrevins on the subcellular localization of IFTB component IFT88, which requires cytoplasmic dynein 2-dependent retrograde transport for its return to the basal body. Treating cells for one hour with ciliobrevin D (**5**) but not DMSO or an inactive analog (**2**) significant increased IFT88 levels at the distal tip of primary cilia (Supplementary Fig. 4), providing further evidence that ciliobrevins inhibit cytoplasmic dynein 2 function.

Cytoplasmic dynein complexes have other cellular functions, including the crosslinking and focusing of microtubule minus ends within the mitotic spindle[3]. These actions create the fusiform shape and localize γ-tubulin-containing complexes to the spindle poles[3]. Cytoplasmic dynein 1 inhibition by blocking antibodies or dominant-negative constructs perturbs spindle assembly, resulting in disorganized poles and reduced γ-tubulin recruitment[3, 12-14]. To determine whether ciliobrevins recapitulate these phenotypes, we treated a metaphase-enriched population of NIH-3T3 cells with 50 μM of either ciliobrevin D (**5**) or an inactive analog (**2**) for one hour and examined their mitotic structures. Cells treated with ciliobrevin D exhibited abnormal (unfocused, multipolar, or collapsed) spindles with disrupted γ-tubulin localization (Fig. 2, a-b, and Supplementary Fig. 5a), while cells incubated with the non-cilia-disrupting analog or vehicle alone exhibited normal spindle morphologies. Similar ciliobrevin-induced spindle defects were observed in HeLa cells, although to a lesser extent (Fig. 2b). Cytoplasmic dynein 1 is also required for establishing stable kinetochore-microtubule interactions[15], and ciliobrevin D treatment disrupted the formation of cold-stable microtubules that mediate proper spindle-chromosome attachments (Fig. 2c).

To investigate if these spindle-disruptive effects were associated with altered dynein localization, we examined binding partners that recruit or co-localize with this motor. Immunofluorescence microscopy showed that p150-Glued, a dynactin component proposed to recruit dynein to kinetochores and spindle poles during mitosis[16], was localized to the disorganized spindle poles of ciliobrevin D-treated cells (Fig. 2d and Supplementary Fig. 5b). Kinetochore targeting of p150-Glued was also unaffected by ciliobrevin D, as assessed in nocodazole-treated cells to obviate effects due to microtubule-attachment status (Supplementary Fig. 6). We similarly observed that Zeste white 10 (Zw10), a component of the Rod/Zw10/Zwilch complex that recruits cytoplasmic dynein 1 to kinetochores[17], and the kinetochore-associated protein Centromere protein E (CENP-E)[18] correctly localized to

kinetochores under these conditions (Supplementary Fig. 6), indicating that their recruitment and kinetochore structure itself are not disrupted by ciliobrevins. Thus, ciliobrevin-induced spindle phenotypes likely result from dynein inhibition rather than mislocalization.

To further characterize the mitotic defects associated with ciliobrevin treatment, we conducted real-time confocal microscopy of GFP-tubulin-expressing NIH-3T3 cells (Supplementary Fig. 7, a-d). Within minutes of ciliobrevin D treatment, spindles collapsed, bipolarity was lost, and spindle poles appeared disorganized. Upon compound washout, bipolar spindles quickly re-emerged and chromosomes segregated at anaphase without any pronounced defects. Ciliobrevin D addition also reversibly disrupted the pre-formed spindles of metaphase-arrested cells (Supplementary Fig. 8, a-c) and reduced overall microtubule levels (Supplementary Fig. 8d). These latter effects are mitosis-specific, as microtubule levels in non-dividing cells were unaffected by inhibitor treatment (Supplementary Fig. 7, e-f). Taken together, these results reveal that cytoplasmic dynein is not only required for spindle pole assembly but also actively participates in its maintenance.

Cytoplasmic dynein 1 also regulates organelle trafficking, such as the melatonin-induced aggregation of melanosomes in *Xenopus* melanophores[19]. To determine if melanosome trafficking is sensitive to ciliobrevins, we cultured *Xenopus* melanophores with melanocyte-stimulating hormone to disperse these pigment granules and then treated the cells with melatonin and various concentrations of ciliobrevin D (**5**) or an inactive analog (**2**). Ciliobrevin D reversibly inhibited melanosome aggregation, but the non-cilia-disrupting derivative had no discernible effect at comparable doses (Fig. 3, a-b, and Supplementary Movies 1-3). Ciliobrevin D similarly abrogated the movement of peroxisomes in *Drosophila* S2 cells (Fig. 3, c-d, and Supplementary Movies 4-5), consistent with the role of cytoplasmic dynein in their bidirectional motility[20].

Collectively, these results indicate that ciliobrevins are specific, reversible inhibitors of disparate cytoplasmic dynein-dependent processes. Ciliobrevins do not perturb cellular mechanisms that are independent of dynein function, including actin cytoskeleton dynamics (Supplementary Fig. 9) and the mitogen-activated protein kinase and phosphoinositol-3-kinase signaling pathways[6]. To more directly examine whether cytoplasmic dynein is the direct target of ciliobrevins, we evaluated their effects on dynein-dependent microtubule gliding *in vitro*. Ciliobrevins A and D (**1** and **5**) retarded the ATP-dependent movement of fluorescently labeled microtubules on bovine cytoplasmic dynein-coated glass slides in a reversible and dose-dependent manner (Fig. 4, a-c, Supplementary Fig. 10, and Supplementary Movies 6-8); analogs that did not perturb cytoplasmic dynein-dependent processes in our cell-based assays (**2** and **8**) had minimal effects (Fig. 4, a-b, and Supplementary Movie 9). The conserved structure-activity-relationships of dihydroquinazolinones in the microtubule gliding and cell-based assays confirm cytoplasmic dynein as the ciliobrevin target, and neither ciliobrevin A nor D significantly affected K560/kinesin-1-dependent microtubule gliding *in vitro* at 100 μM concentrations (Fig. 4d and Supplementary Movies 10-12). The compounds do not broadly target members of the AAA+ ATPase family either, as they have no effect on p97-dependent degradation of endoplasmic reticulum-associated proteins (Supplementary Fig. 11) or Mcm2-7-mediated DNA unwinding (Supplementary Fig. 12).

We next investigated how ciliobrevins abrogate cytoplasmic dynein function. Neither ciliobrevin A nor D was able to disrupt the association between ADP-bound dynein and microtubules, as determined in a co-sedimentation assay (Supplementary Fig. 13). Both small molecules, however, were able to inhibit the ATPase activity of bovine brain cytoplasmic dynein in a concentration-dependent manner, while their inactive analog (**2**) could not (Supplementary Fig. 14). The compounds had analogous effects on the ATPase activity of recombinant rat dynein motor domain, but none significantly inhibited the ATPase activities of recombinant motor domains derived from human kinesin-1 or kinesin-5 (Fig. 4e). Ciliobrevin efficacies at various ATP concentrations suggest that these small molecules act in a nucleotide-competitive manner (Fig. 4f). Consistent with this mechanism, ciliobrevin A also inhibited ultraviolet light-induced cleavage of the cytoplasmic dynein motor domain in the presence of sodium vanadate and ATP (Supplementary Fig. 15).

Our studies establish ciliobrevins as the first small molecules known to specifically inhibit cytoplasmic dynein *in vitro* and in live cells. Although the ATP analog erythro-9-[3-(2-hydroxynonyl)]adenine[21] and the antioxidant nordihydroguaiaretic acid[22] have been previously reported to abrogate dynein function, these compounds are promiscuous enzyme antagonists[23,24]. The natural product purealin can partially inhibit dynein ATPase activity *in vitro*[25], but its ability to block cytoplasmic dynein-dependent cellular processes has not been demonstrated. Our studies indicate that ciliobrevins can inhibit both cytoplasmic dynein 1 and 2, and accordingly, the compounds will be broadly applicable probes of dynein-dependent processes. Further development of ciliobrevin-like molecules could lead to isoform-selective inhibitors of this minus-end directed microtubule motor and perhaps specific antagonists of other AAA+ ATPase superfamily members.

Methods Summary

Hh signaling assays

Hh signaling and Gli3 processing assays were performed as described[6,9].

Cell imaging

Cilia were immunostained with anti-Arl13b antibody (T. Caspary), and cilia size was determined by dividing the number of Arl13b-positive pixels by the number of nuclei per image. Ciliary levels of Gli2 and IFT88 were determined by immunostaining cells with anti-Gli2 (R&D Systems) or anti-IFT88 (ProteinTech Group) antibodies. Analyses of mitotic spindles and kinetochore-microtubule attachments in fixed cells were performed as described[26], and real-time confocal microscopy was conducted with NIH-3T3 cells stably expressing GFP-tubulin. Melanosome and peroxisome motility studies were conducted as reported[19,20].

Dynein activity assays

Bovine brain dynein was purified as described[27], and its microtubule gliding activity was assayed as reported[28] with modifications. Recombinant rat cytoplasmic dynein motor domain was heterologously expressed and purified as described[29]. ATPase activities were determined using a Malachite Green assay (Novus Biologicals).

Full Methods

Full Methods and any associated references are available in Supplementary Information.

Supplementary Material

Refer to Web version on PubMed Central for supplementary material.

Acknowledgments

We thank T. Caspary for anti-Arl13b antibodies, W. Brinkley for human CREST anti-serum, T. Yen for anti-CENP-E antibodies, U. Peters for purified bovine dynein, S. Wacker for human kinesin-5 motor domain, R. Vallee for a pVL1393 baculovirus expression vector containing the rat dynein motor domain, and K. Bersuker and R. Kopito for TCRα-GFP-expressing cells. This work was supported by funding from the National Institutes of Health (R01 CA136574 to J.K.C.; R01 GM65933 to T.M.K; R01 GM71772 to T.M.K. and V.I.G.; R01 GM52111 to V.I.G.)

References

1. White SR, Lauring B. AAA+ ATPases: achieving diversity of function with conserved machinery. Traffic. 2007; 8:1657–1667. [PubMed: 17897320]
2. Scholey JM. Intraflagellar transport. Annu Rev Cell Dev Biol. 2003; 19:423–443. [PubMed: 14570576]
3. Merdes A, Ramyar K, Vechio JD, Cleveland DW. A complex of NuMA and cytoplasmic dynein is essential for mitotic spindle assembly. Cell. 1996; 87:447–458. [PubMed: 8898198]
4. Akhmanova A, Hammer JA 3rd. Linking molecular motors to membrane cargo. Curr Opin Cell Biol. 2010; 22:479–487. [PubMed: 20466533]
5. Chou TF, et al. Reversible inhibitor of p97, DBeQ, impairs both ubiquitin-dependent and autophagic protein clearance pathways. Proc Natl Acad Sci U S A. 2011; 108:4834–4839. [PubMed: 21383145]
6. Hyman JM, et al. Small-molecule inhibitors reveal multiple strategies for Hedgehog pathway blockade. Proc Natl Acad Sci U S A. 2009; 106:14132–14137. [PubMed: 19666565]
7. Jiang J, Hui CC. Hedgehog signaling in development and cancer. Dev Cell. 2008; 15:801–812. [PubMed: 19081070]
8. Goetz SC, Anderson KV. The primary cilium: a signalling centre during vertebrate development. Nat Rev Genet. 2010; 11:331–344. [PubMed: 20395968]
9. Humke EW, Dorn KV, Milenkovic L, Scott MP, Rohatgi R. The output of Hedgehog signaling is controlled by the dynamic association between Suppressor of Fused and the Gli proteins. Genes Dev. 2010; 24:670–682. [PubMed: 20360384]
10. Kim J, Kato M, Beachy PA. Gli2 trafficking links Hedgehog-dependent activation of Smoothened in the primary cilium to transcriptional activation in the nucleus. Proc Natl Acad Sci U S A. 2009; 106:21666–21671. [PubMed: 19996169]
11. Huangfu D, Anderson KV. Cilia and Hedgehog responsiveness in the mouse. Proc Natl Acad Sci U S A. 2005; 102:11325–11330. [PubMed: 16061793]
12. Heald R, et al. Self-organization of microtubules into bipolar spindles around artificial chromosomes in Xenopus egg extracts. Nature. 1996; 382:420–425. [PubMed: 8684481]
13. Gaglio T, Dionne MA, Compton DA. Mitotic spindle poles are organized by structural and motor proteins in addition to centrosomes. J Cell Biol. 1997; 138:1055–1066. [PubMed: 9281583]
14. Young A, Dictenberg JB, Purohit A, Tuft R, Doxsey SJ. Cytoplasmic dynein-mediated assembly of pericentrin and gamma tubulin onto centrosomes. Mol Biol Cell. 2000; 11:2047–2056. [PubMed: 10848628]
15. Varma D, Monzo P, Stehman SA, Vallee RB. Direct role of dynein motor in stable kinetochore-microtubule attachment, orientation, and alignment. J Cell Biol. 2008; 182:1045–1054. [PubMed: 18809721]

16. King SJ, Brown CL, Maier KC, Quintyne NJ, Schroer TA. Analysis of the dynein-dynactin interaction in vitro and in vivo. Mol Biol Cell. 2003; 14:5089–5097. [PubMed: 14565986]
17. Starr DA, Williams BC, Hays TS, Goldberg ML. ZW10 helps recruit dynactin and dynein to the kinetochore. J Cell Biol. 1998; 142:763–774. [PubMed: 9700164]
18. Yen TJ, Li G, Schaar BT, Szilak I, Cleveland DW. CENP-E is a putative kinetochore motor that accumulates just before mitosis. Nature. 1992; 359:536–539. [PubMed: 1406971]
19. Gross SP, et al. Interactions and regulation of molecular motors in Xenopus melanophores. J Cell Biol. 2002; 156:855–865. [PubMed: 11864991]
20. Kim H, et al. Microtubule binding by dynactin is required for microtubule organization but not cargo transport. J Cell Biol. 2007; 176:641–651. [PubMed: 17325206]
21. Bouchard P, Penningroth SM, Cheung A, Gagnon C, Bardin CW. erythro-9-[3-(2-Hydroxynonyl)]adenine is an inhibitor of sperm motility that blocks dynein ATPase and protein carboxylmethylase activities. Proc Natl Acad Sci U S A. 1981; 78:1033–1036. [PubMed: 6453342]
22. Arasaki K, Tani K, Yoshimori T, Stephens DJ, Tagaya M. Nordihydroguaiaretic acid affects multiple dynein-dynactin functions in interphase and mitotic cells. Mol Pharmacol. 2007; 71:454–460. [PubMed: 17105871]
23. Schliwa M, Ezzell RM, Euteneuer U. erythro-9-[3-(2-Hydroxynonyl)]adenine is an effective inhibitor of cell motility and actin assembly. Proc Natl Acad Sci U S A. 1984; 81:6044–6048. [PubMed: 6385006]
24. Park S, Lee DK, Yang CH. Inhibition of fos-jun-DNA complex formation by dihydroguaiaretic acid and in vitro cytotoxic effects on cancer cells. Cancer Lett. 1998; 127:23–28. [PubMed: 9619854]
25. Zhu G, et al. Synthesis and biological evaluation of purealin and analogues as cytoplasmic dynein heavy chain inhibitors. J Med Chem. 2006; 49:2063–2076. [PubMed: 16539395]
26. Maldonado M, Kapoor TM. Constitutive Mad1 targeting to kinetochores uncouples checkpoint signalling from chromosome biorientation. Nat Cell Biol. 2011; 13:475–482. [PubMed: 21394085]
27. Woehlke G, et al. Microtubule interaction site of the kinesin motor. Cell. 1997; 90:207–216. [PubMed: 9244295]
28. Kapoor TM, Mitchison TJ. Allele-specific activators and inhibitors for kinesin. Proc Natl Acad Sci U S A. 1999; 96:9106–9111. [PubMed: 10430903]
29. Hook P, et al. Long range allosteric control of cytoplasmic dynein ATPase activity by the stalk and C-terminal domains. J Biol Chem. 2005; 280:33045–33054. [PubMed: 16030013]
30. Taipale J, et al. Effects of oncogenic mutations in Smoothened and Patched can be reversed by cyclopamine. Nature. 2000; 406:1005–1009. [PubMed: 10984056]

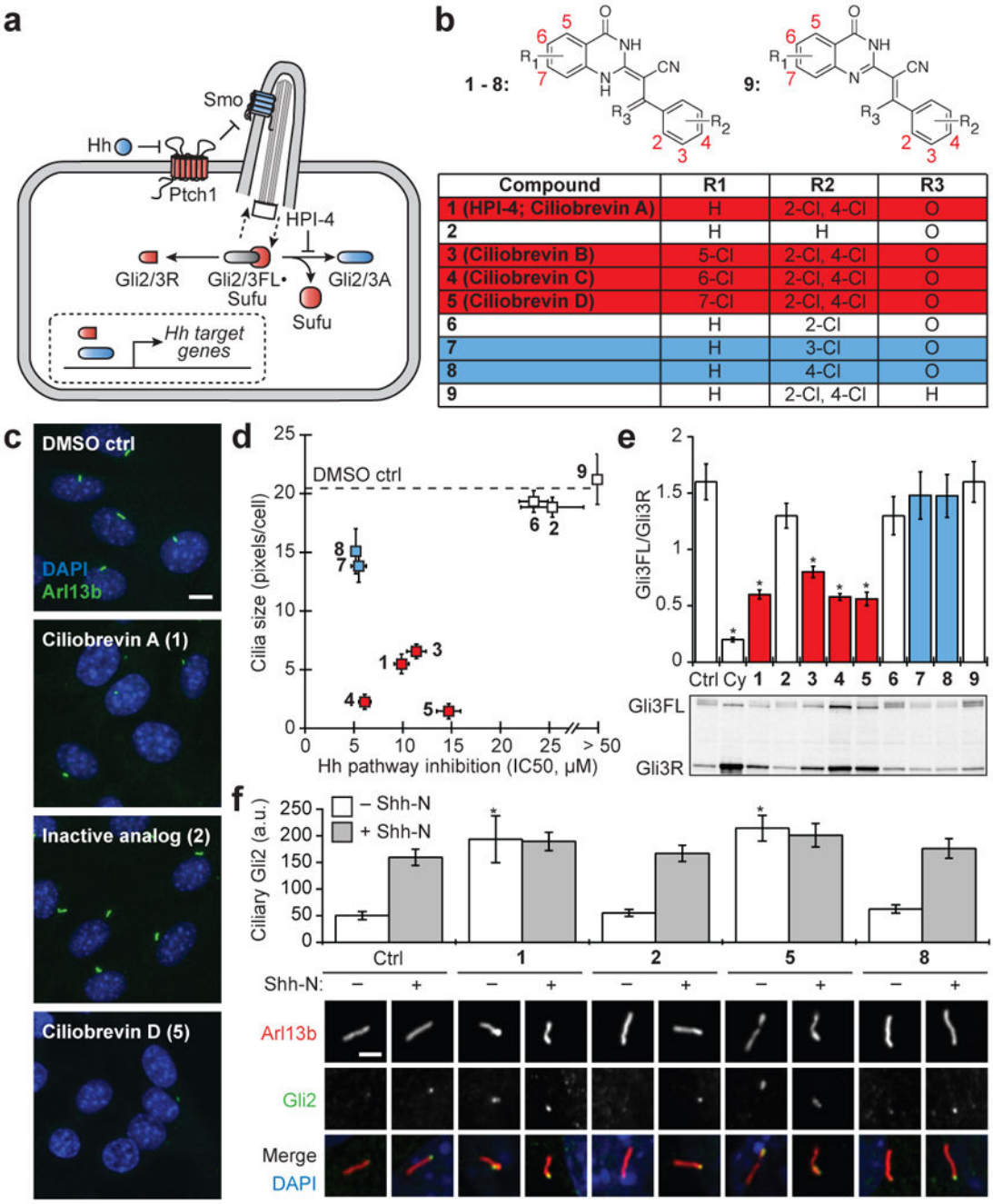

Compound	R1	R2	R3
1 (HPI-4; Ciliobrevin A)	H	2-Cl, 4-Cl	O
2	H	H	O
3 (Ciliobrevin B)	5-Cl	2-Cl, 4-Cl	O
4 (Ciliobrevin C)	6-Cl	2-Cl, 4-Cl	O
5 (Ciliobrevin D)	7-Cl	2-Cl, 4-Cl	O
6	H	2-Cl	O
7	H	3-Cl	O
8	H	4-Cl	O
9	H	2-Cl, 4-Cl	H

Figure 1. Ciliobrevins disrupt primary cilium-dependent Gli regulation

a, Depiction of Hh signaling with positive (blue) and negative (red) regulators. **b**, Dihydroquinazolinone structures. **c**, Ciliary phenotypes after treatment with individual compounds (30 μM) for 24 hours. Scale bar, 10 μm. **d**, Compound effects on Hh target gene expression in Shh-LIGHT2 cells[30] and cilia size in Shh-EGFP cells[6]. IC_{50}'s are the average of three independent experiments ± s.d., and cilia size is defined as the average number of Arl13b-positive pixels per nuclei for ten micrographs ± s.d., each containing approximately 150 cells. Small molecules that block Hh signaling alone (blue) and those that inhibit both Hh pathway activity and ciliogenesis (ciliobrevins; red) are highlighted. **e**, Gli3FL and

Gli3R levels in Shh-EGFP cells treated with Shh-N and either individual dihydroquinazolinones (30 μM), 3 μM cyclopamine, or DMSO for 16 hours. Average Gli3FL/Gli3R ratios for five independent experiments ± s.e.m. and a representative immunoblot are shown, with asterisks indicating $p < 0.005$ for individual compounds vs. DMSO. **f**, Ciliary Gli2 levels in Shh-EGFP cells treated with selected ciliobrevins (**1** and **5**), inactive analogs (**2** and **8**), or DMSO for 4 hours. Average Gli2 levels in the distal end of at least 25 cilia ± s.e.m. and representative confocal micrographs are shown. Asterisks indicate $p < 0.005$ for individual compounds vs. DMSO. Scale bar, 1 μm.

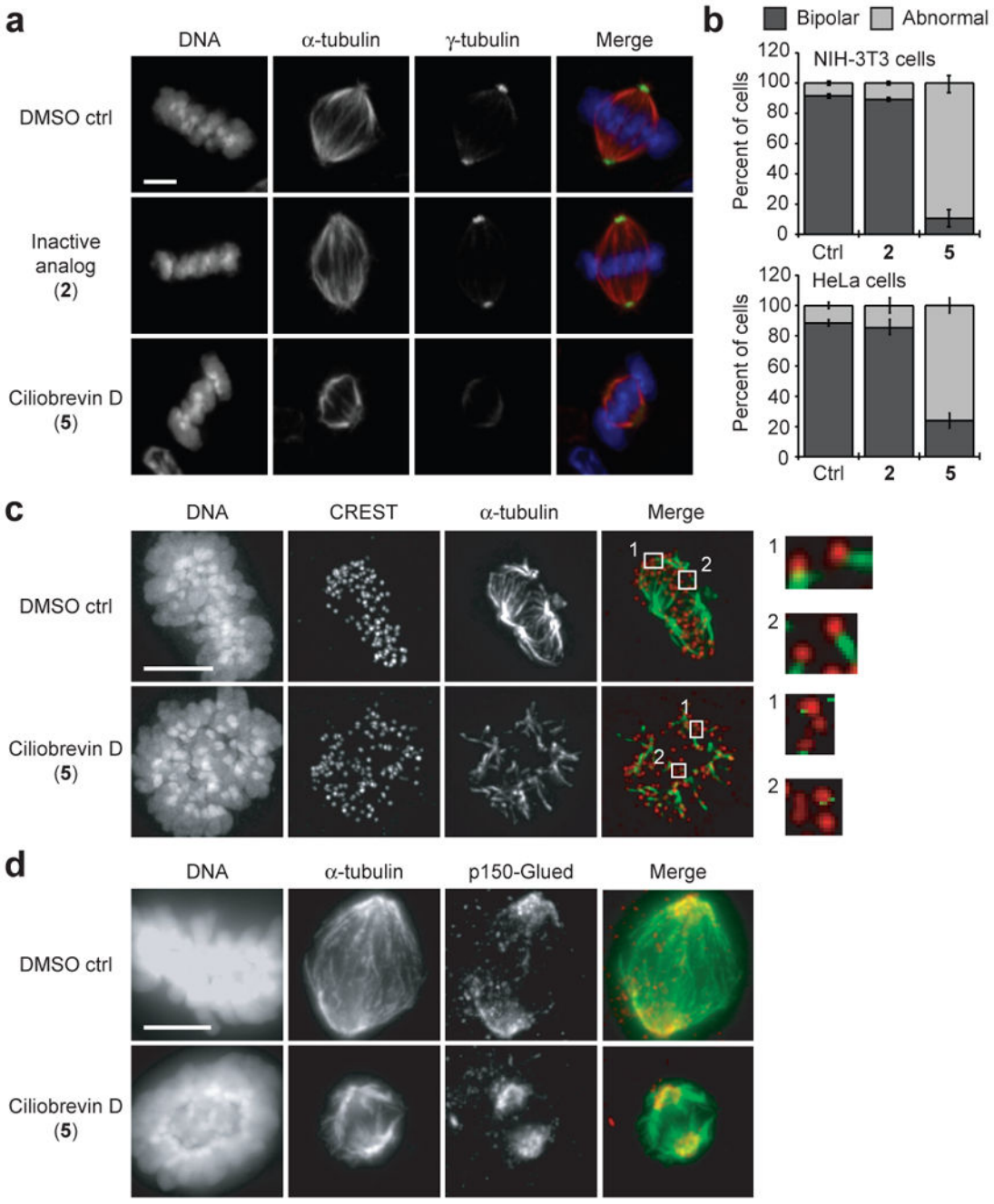

Figure 2. Ciliobrevins disrupt spindle pole assembly and kinetochore-microtubule attachment

a, Mitotic spindles observed in NIH-3T3 cells treated with MG132 for 90 min and subsequently cultured with an inactive analog (**2**) or ciliobrevin D (**5**) at a 50-μM dose or DMSO for 1 hour. Staining for DNA, α-tubulin, and γ–tubulin are shown. **b**, Quantification of spindle phenotypes in NIH-3T3 and HeLa cells treated as described above and scored for either bipolar or abnormal morphologies. Data are the average of three independent experiments ± s.e.m., each including at least 150 spindles. **c**, Kinetochore-microtubule interactions analyzed in metaphase-arrested NIH-3T3 cells treated with DMSO or 50 μM **5** and then incubated on ice for 10 min. Staining for DNA, the kinetochore marker CREST,

and α-tubulin are shown. Insets highlight individual kinetochore-microtubule attachments or untethered kinetochores (400% magnification). **d**, Localization of p150-Glued in metaphase-arrested NIH-3T3 cells treated with DMSO or 50 μM **5**. Staining for DNA, α-tubulin, and p150-Glued are shown. Scale bars: **a**, 4 μm; **c**-**d**, 5 μm.

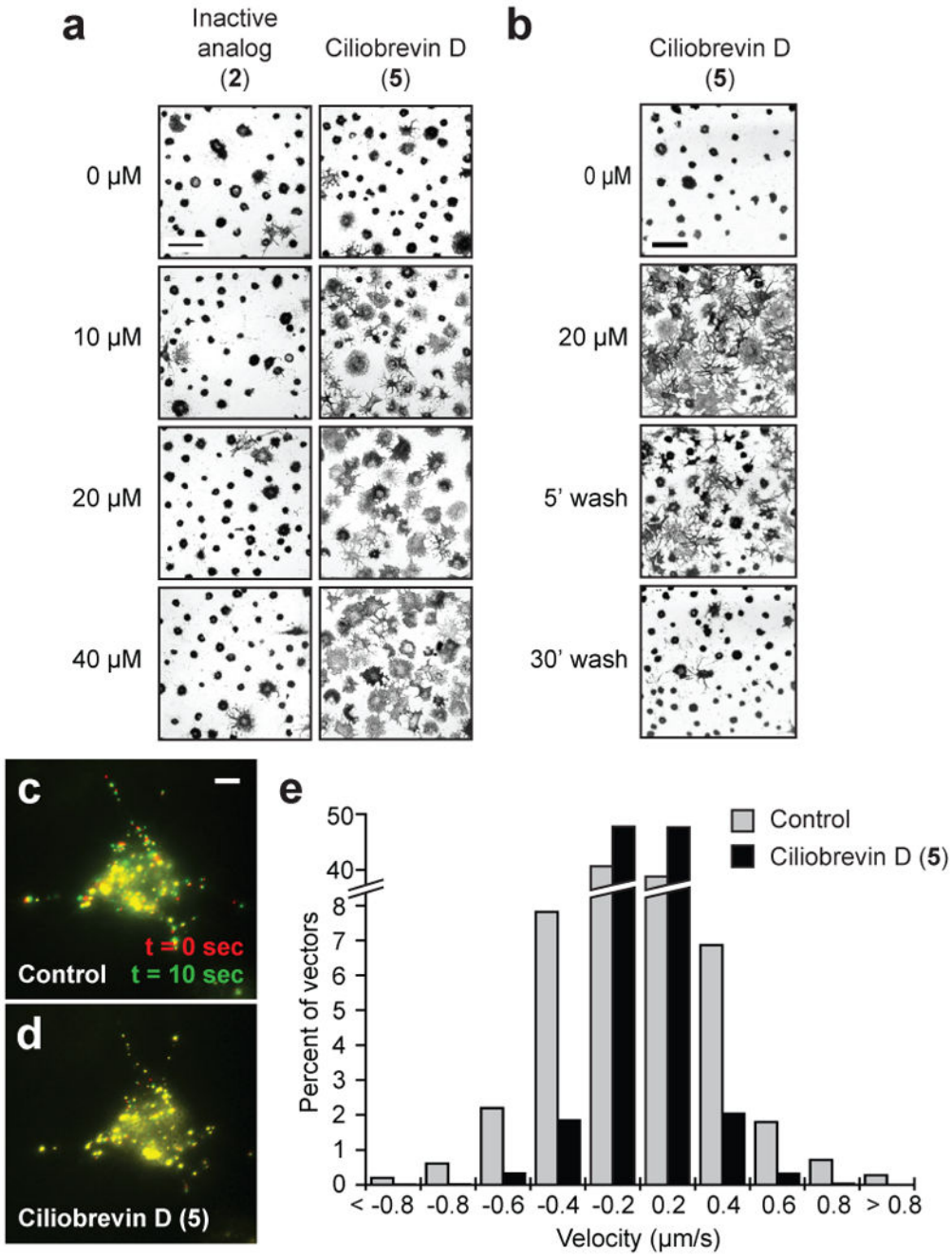

Figure 3. Ciliobrevins inhibit melanosome aggregation and peroxisome motility

a, Brightfield images of *Xenopus* melanophores treated with various concentrations of ciliobrevin D (**5**) or an inactive derivative (**2**) for 10 min, stimulated with melatonin for 30 min, and then paraformaldehyde-fixed. **b**, Melanophores treated with **5** as before, washed in medium containing melatonin alone, and then imaged. Scale bars, 100 μm. **c-d**, Motility of GFP-labeled peroxisomes in *Drosophila* S2 cells cultured in the absence (**c**) or presence (**d**) of **5**. Overlays of videomicroscopy frames at t = 0 seconds (red) and t = 10 seconds (green) are shown. Scale bar, 5 μm. **e**, Vector distributions for the GFP-labeled peroxisomes with

movement toward and away from the cell center denoted by negative and positive bin values, respectively.

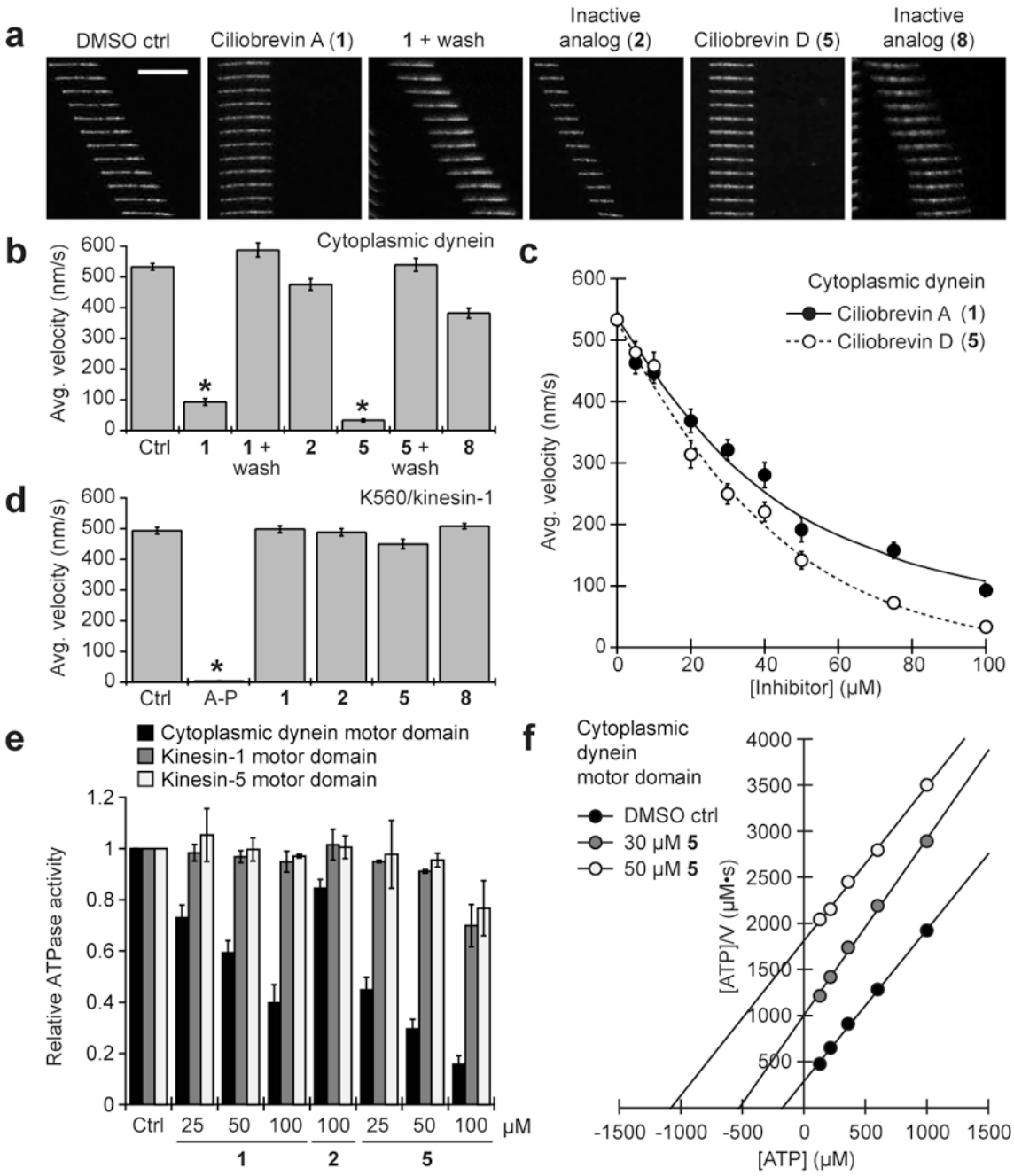

Figure 4. Ciliobrevins inhibit cytoplasmic dynein-dependent microtubule gliding and ATPase activity

a, Kymographs of fluorescent microtubules moving on bovine dynein-coated glass slides in the presence of ATP and either DMSO, ciliobrevin A (**1**), ciliobrevin D (**5**), or non-cilia-disrupting analogs (**2** and **8**). All compounds were tested at a 100-μM concentration, and each vertical frame represents 2 seconds. Scale bar, 10 μm. **b**, Quantification of the compounds' effects on dynein-dependent microtubule gliding. Data are the average velocities for at least 56 microtubules ± s.e.m. Asterisks indicate $p < 10^{-6}$ and at least 30% inhibition for individual compounds vs. DMSO. **c**, Dose responses of **1** and **5** in the dynein-

dependent assay. Data are the average velocities for at least 45 microtubules ± s.e.m. **d**, Effects of **1, 2, 5, 8**, and the competitive ATP antagonist adenylyl imidodiphosphate (AMP-PNP) on microtubule gliding driven by the K560 N-terminal fragment of kinesin-1. Dihydroquinazolinones and AMP-PNP were tested at a 100-μM and 1-mM concentrations, respectively. Data are the average velocities for at least 34 microtubules ± s.e.m., and asterisks indicate $p < 0.01$ for individual compounds vs. DMSO. **e**, Effects of **1, 2**, and **5** on the ATPase activities of recombinant motor domains derived from rat cytoplasmic dynein, human kinesin-1, and human kinesin-5. Compound concentrations in micromolar units are shown, and data are the average ATPase activities for two independent experiments ± s.d. **f**, Hanes-Woolf plot of rat dynein motor ATPase kinetics demonstrating the nucleotide-competitive activity of **5**.